Seismic Imaging of Shallow Crustal Structure in Northern California Using Ambient-noise-derived Rayleigh Wave Ellipticity and Receiver Functions

G. Zaldívar[1], H. Kim[1], F.-C. Lin[1] and T. Taira[2] (1: University of Utah, 2:Berkeley Seismological Laboratory)

Summary

- Northern California contains numerous active faults, including the Hayward Fault near the San Francisco Bay Area, which is capable of generating large-magnitude (M > 6) earthquakes with potentially severe impacts. Accurate three-dimensional (3D) seismic velocity models, particularly those that capture detailed uppermost crustal structure, are crucial for predicting ground motions during such events.
- Given the high population at San Francisco Bay Area, which is exposing a high probability of seismic hazard, there have been considerable efforts to develop a 3D velocity model mainly led by USGS. Based on geological information, the first detailed 3D velocity model was developed. This model has served as a Community Velocity Model (CVM), and earthquake ground-motion simulation analyses have been incorporated into this CVM.
- We performed Rayleigh wave ellipticity measurements and Receiver function first peak delay time measurements using stations in Northern and Central California. Both measurements exhibit variations that reflect the existence of sedimentary basins in the area.
- A comparison of the observations to the predictions of the community velocity model shows large-scale agreement in areas of high and low values but also shows difference within areas of high and low values.
- The discrepancy is prominent within the Central Valley and Sacramento-San Joaquin Delta, that the predictions from the model are always lower than the observations. This implies that the community velocity model has the potential to be further improved to explain the seismic data sets better.
- Future directions of research should be inverting the seismic observations to velocity models and incorporating them into the next version of the CVM.

Community Velocity Model (CVM)

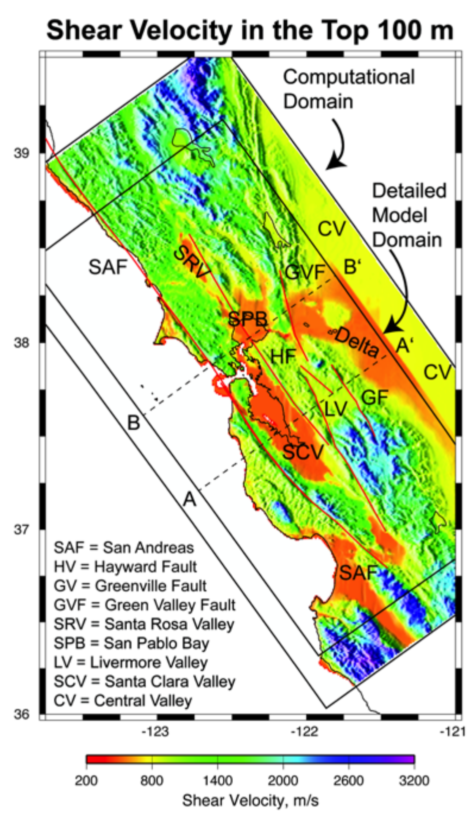

- USGS SFBA CVM built from geologic and geophysical constraints
- Rocks east of the HF are composed of basement comprising the sedimentary Great Valley Complex
- Rocks to the west of the HF they are predominantly the Franciscan Complex
- This heterogeneity results in much lower upper crustal wave speeds for the Great Valley Complex than the Franciscan Complex

Figure 1: USGS 3D seismic velocity model (version USGSBayAreaVM-08.3.0.etree)

Seismic Data and Noise Correlation Measurements

Northern California Seismic Stations

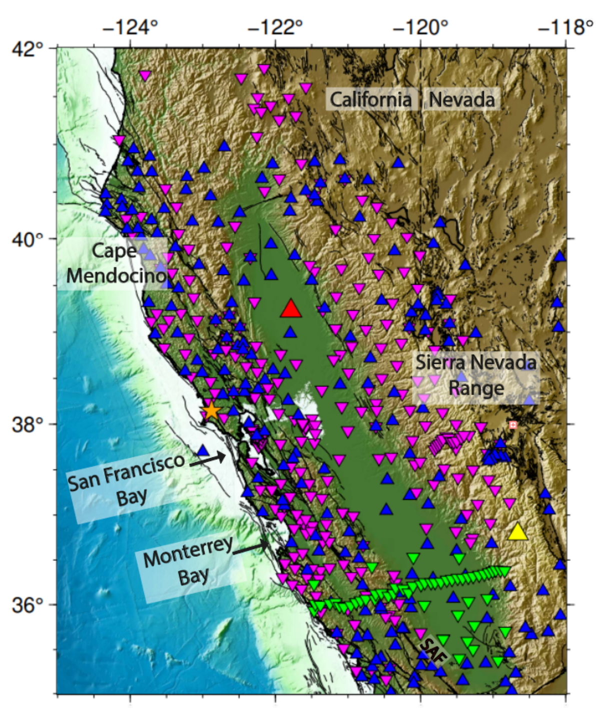

Figure 2: Location map of the imaged region. Stations used for HV analysis (blue triangles), additional stations used for RF analysis (magenta inverted triangles), TO array (green inverted triangles), faults, and topography. The orange star marks the location of the station used in the record plot in Figure 2. Example stations BK.CGRV (yellow triangle) and BK.SUTB (red triangle) used in Figure 3 are marked. TO stations CC04, CC22, and CC25 used in Figure 7 & 8 are also identified.

- Ambient-noise Green's functions (GFs) and theoretical GFs, calculated using SW4 (4th order finite difference code) in GIL7 (1D velocity model) and the USGS 3D SFBA velocity model for BDSN broadband seismic stations

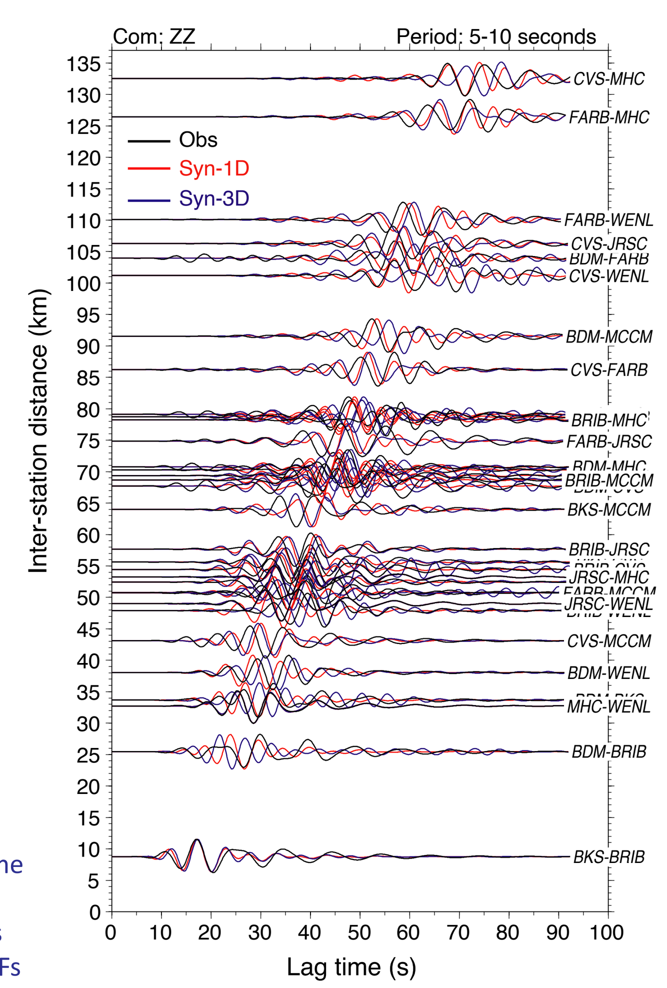

Figure 3: Comparisons of the vertical velocity waveforms using the GFs from ambient noise cross-correlations (black). Also shows are SW4-synthetic GFs for the 1D GIL7 (red) and the USGS SFBA 3D velocity model. All data are band-pass filtered between 10s-20s. Amplitudes are normalized.

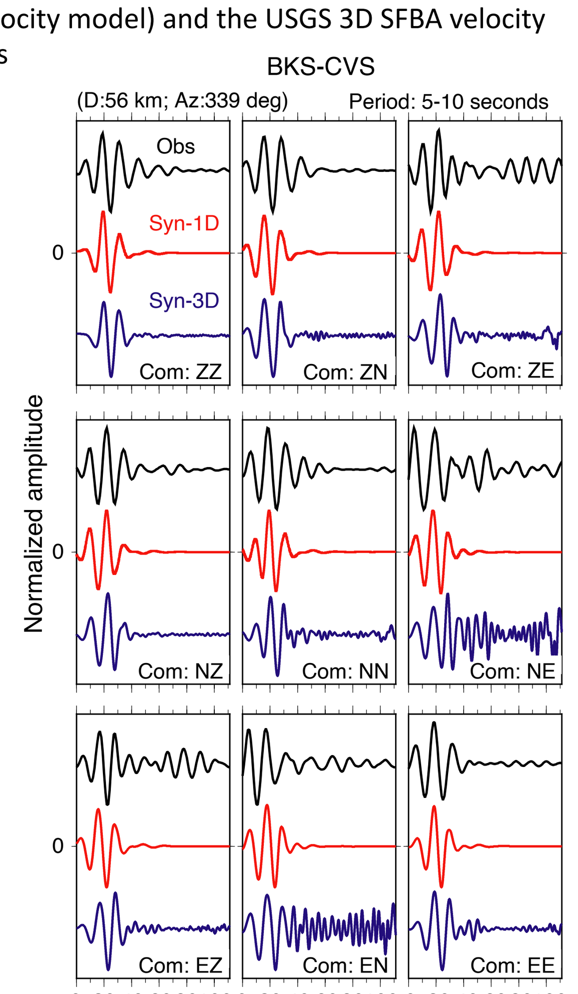

Figure 4: 9-component GFs from ambient noise cross-correlations (black) for BK.BKS-BK.CVS. Also shows are SW4-synthetic GFs for the 1D GIL7 (red) and the USGS SFBA 3D velocity model. All data are band-pass filtered between 10s-20s. Amplitudes are normalized.

Evaluating Path-Specific Bias in CVM

- For Obs-Syn3D comparison, ray paths propagating the east side of HF show a positive time lag, suggesting that the SFBA 3D Velocity model generates velocities that are too slow.

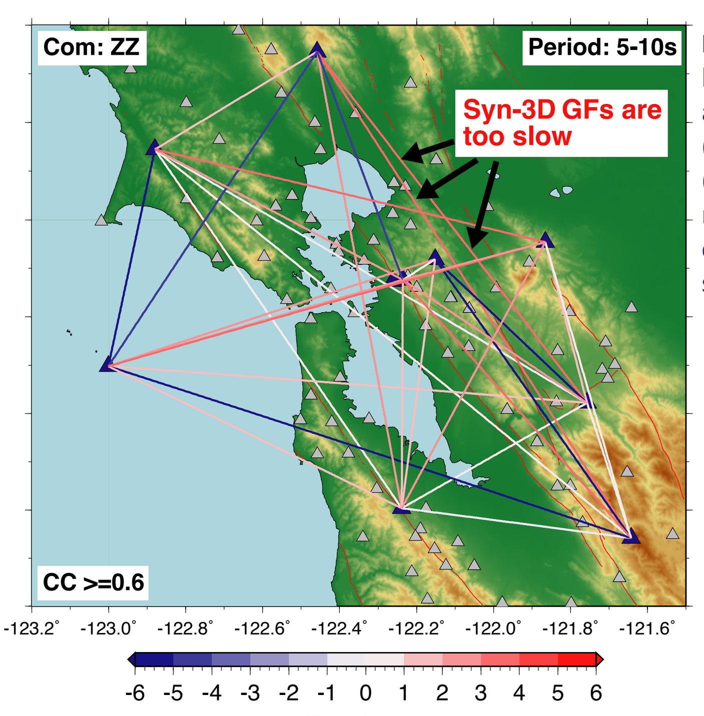

Figure 5: Ray paths and time lags between the ambient-noise derived GFs (obs) and SW4 synthetic GFs (Syn-3D). Only paths with normalized cross-correlation coefficient above 0.6 are shown.

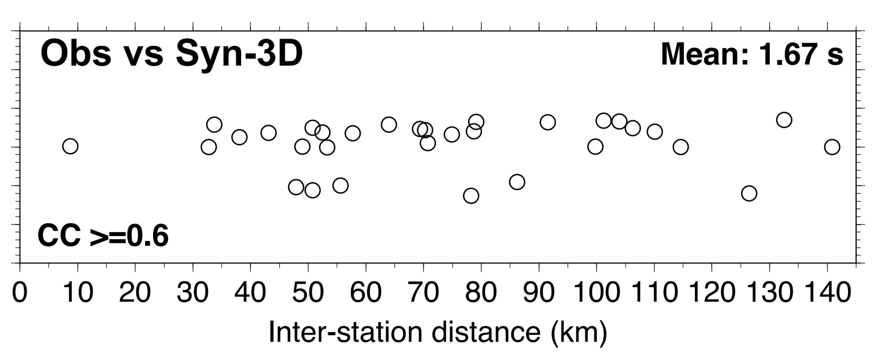

Figure 6: Time lag measurement between observed and Syn-3D GFs as a function of interstation distance. Only time-lag data with normalized cross-correlation coefficient above 0.6 are shown.

Rayleigh Wave Ellipticity (H/V Ratio)

Multi-Component Cross Correlations

- Computed 9-component ambient noise CC's, rotated into R and T components.
- HV Extracted using Frequency-Time Analysis (FTAN).
- Higher H/V values in basins indicate strong horizontal motion.
- Lower values in mountains suggest dominant vertical motion.

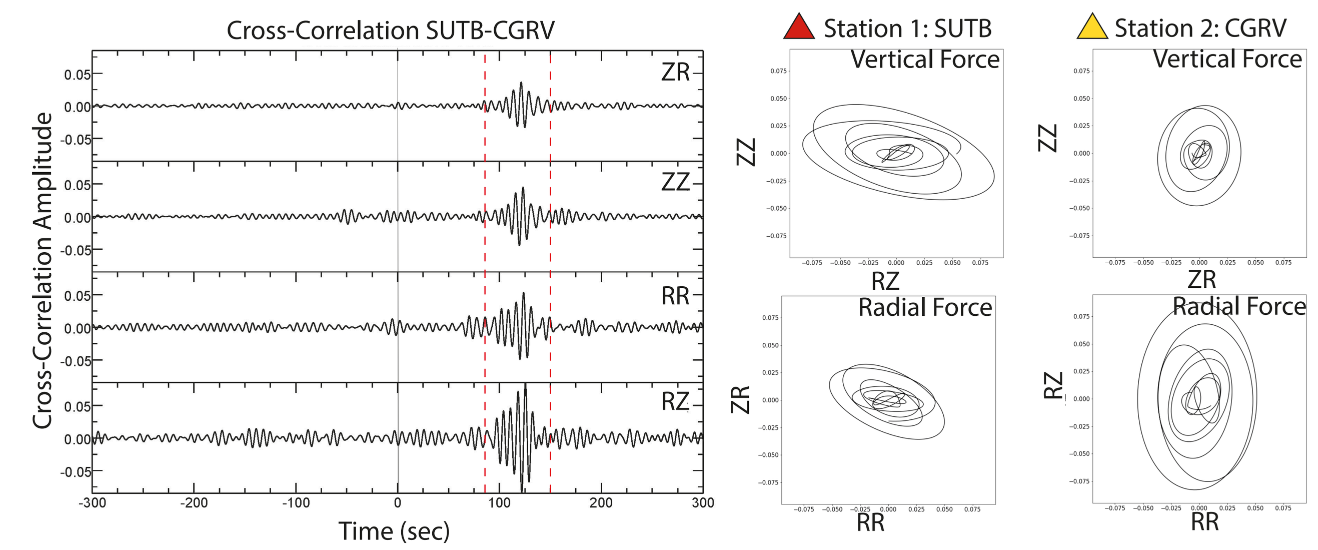

Figure 7: Multi-component ambient noise cross- correlations between stations BK.SUTB and BK.CGRV filtered between 5 and 10 s. Rayleigh waves are visible on all components (Z: vertical; R: radial). The Rayleigh wave particle motions at CGRV and SUTB excited by both vertical and radial force components are also shown.

Comparison of Observations with Predictions using USGS_SVM

- High H/V values are observed within the major basin environment such as Central Valley.

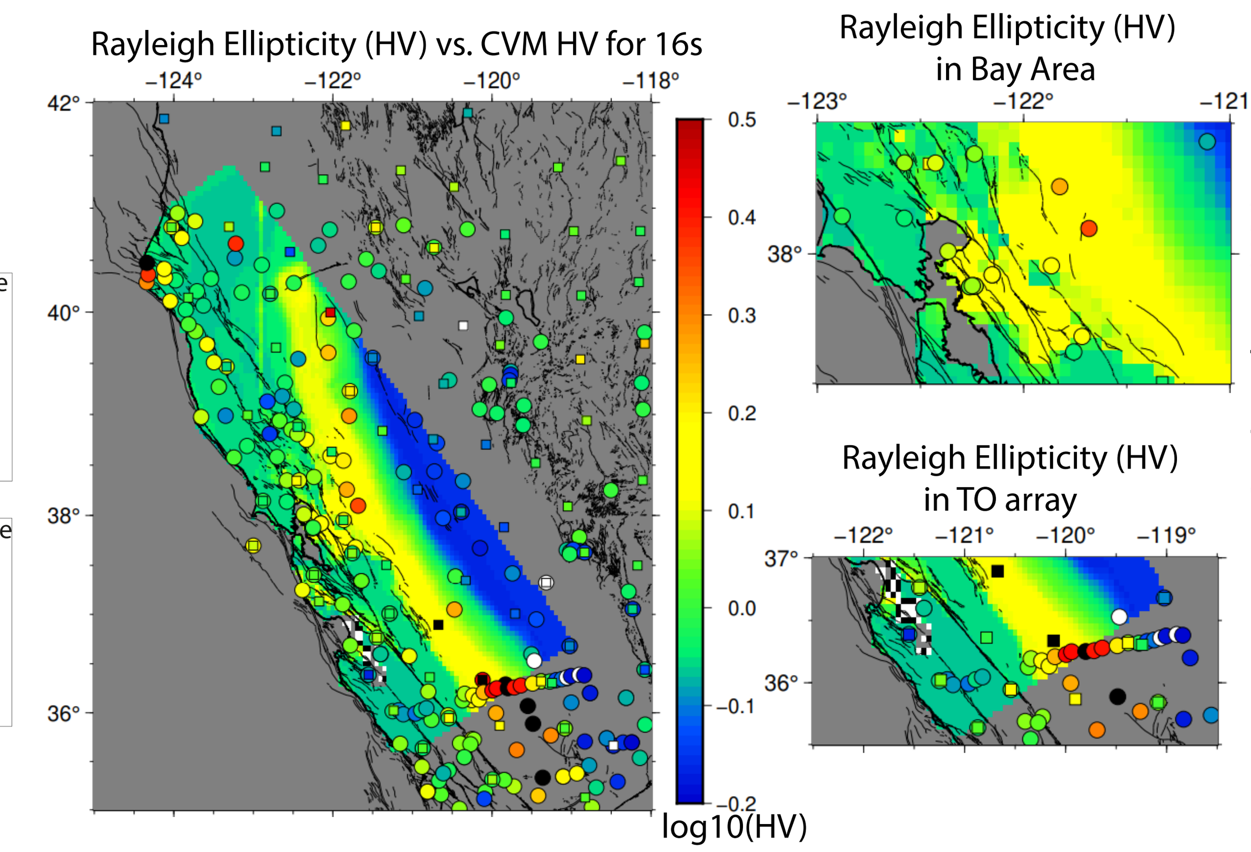

Figure 8: H/V map displaying individual station results (circles) alongside USArray results (squares), overlaid on predicted H/V values from USGS_SVM in the background. (left) The entire area. (upper right) Zoom into the Bay area. (lower left) Zoom into southern Central Valley.

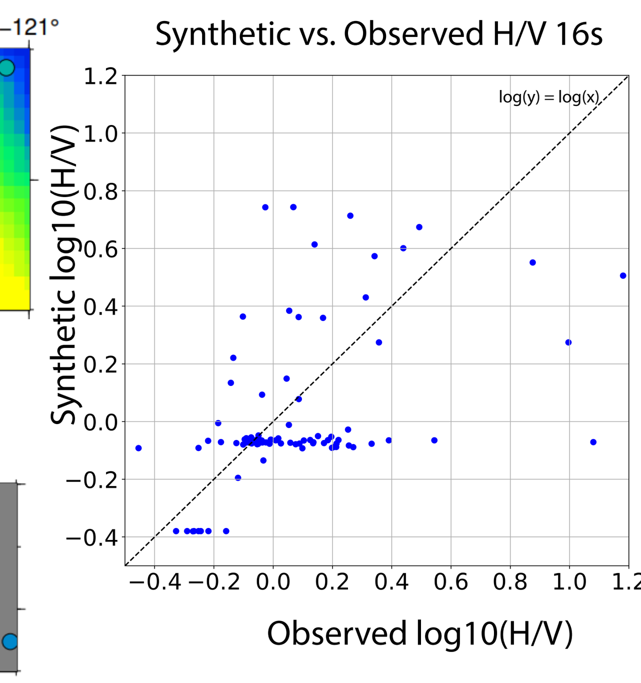

Figure 9: Scatter plot between the observed and CVM predicted 16 sec Rayleigh wave H/V ratios.

Receiver Function Analysis

Initial Peak Delay Time in Teleseismic P-wave Receiver Function (RF)

- Uses teleseismic P-waves from earthquakes (M ≥ 5.8, 25°–90°) between 2014–2024. RFs extracted by deconvolving vertical from radial components, filtering for high signal-to-noise ratios. First peak delay time highlights sediment thickness, stacking RFs enhances robustness.

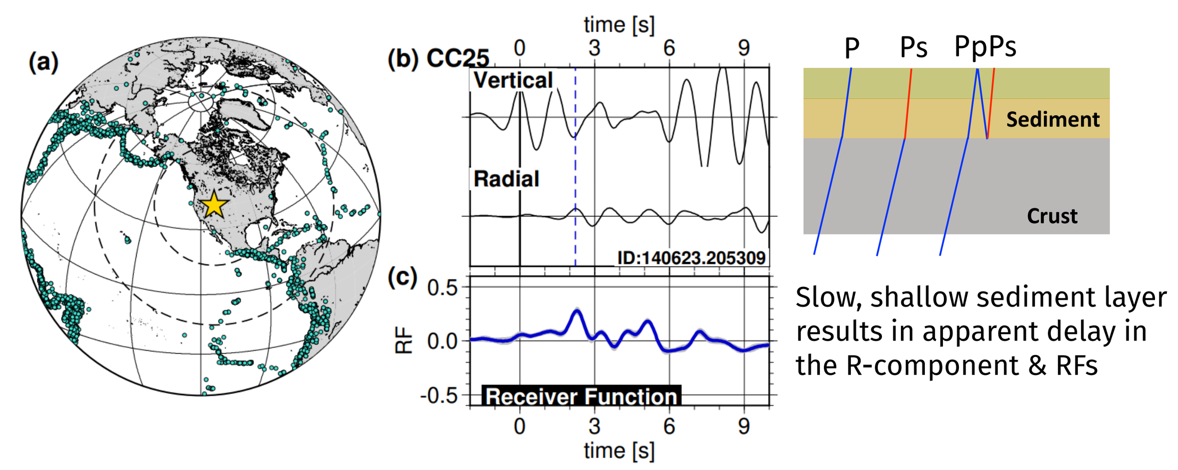

Figure 10: (a) Map of teleseismic earthquakes used in our RF analysis. (b) Example seismic data for estimating P-wave RF and (b) resultant RF.

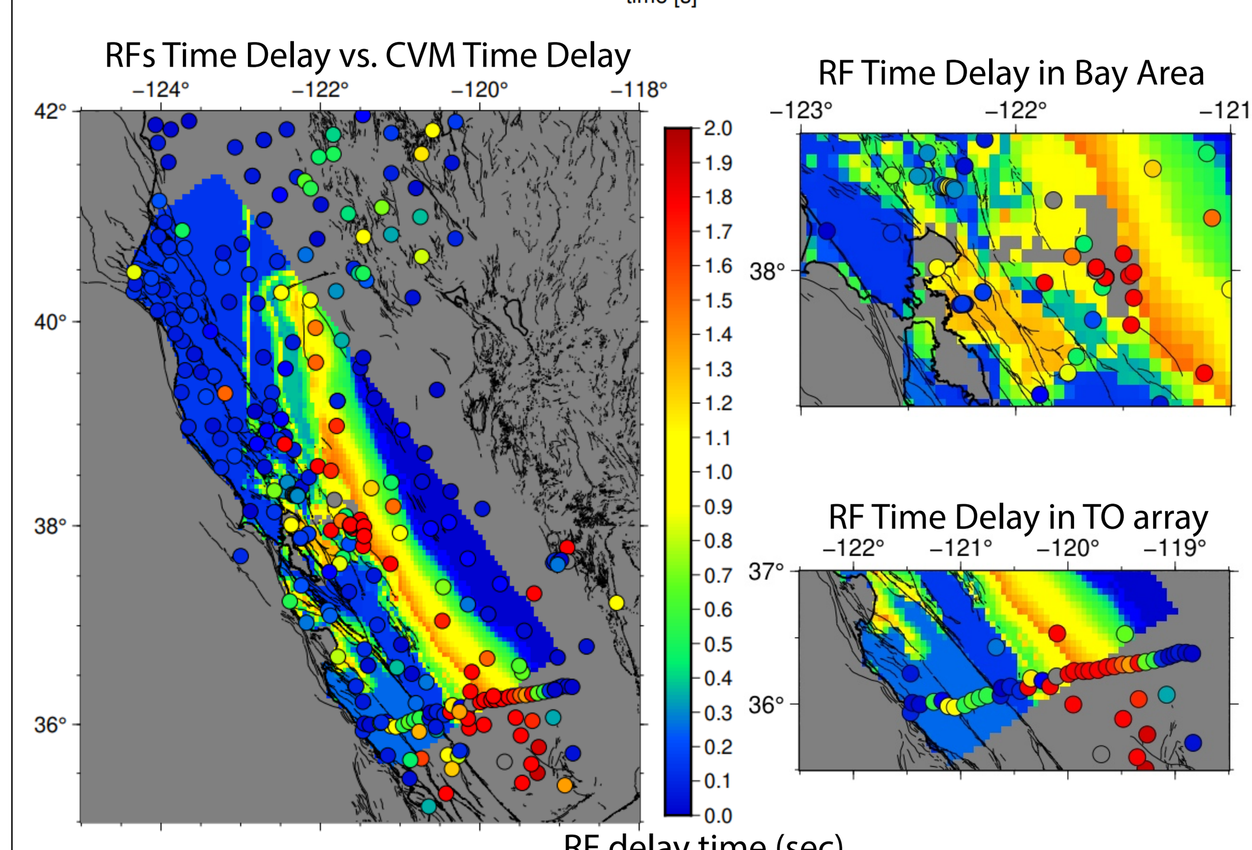

Figure 11: Map of RF delay time displaying individual station results (circles) alongside USArray results (squares), overlaid on predicted H/V values from USGS_SVM in the background. (left) The entire area. (upper right) Zoom into the Bay area. (lower left) Zoom into southern Central Valley.

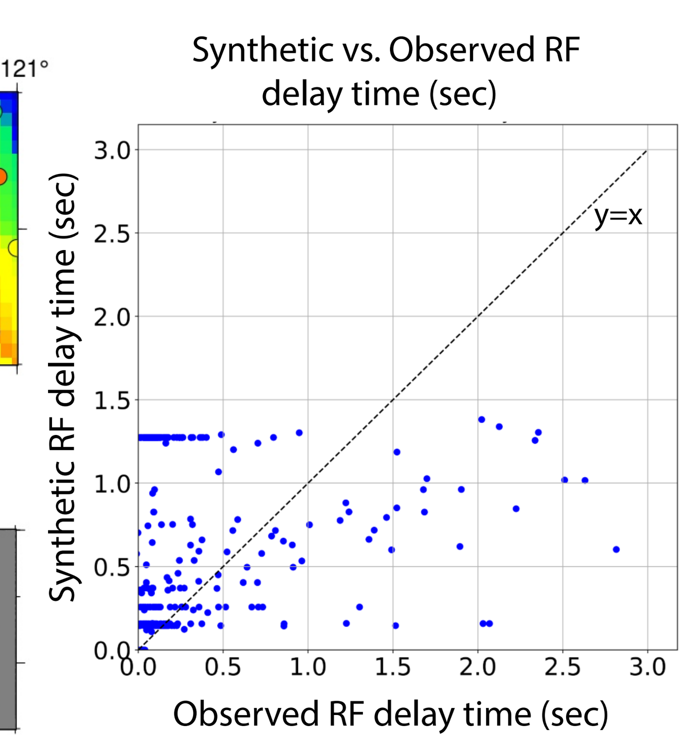

Figure 12: Scatter plot between the observed and CVM predicted RF delay times.

Joint Seismic Inversion

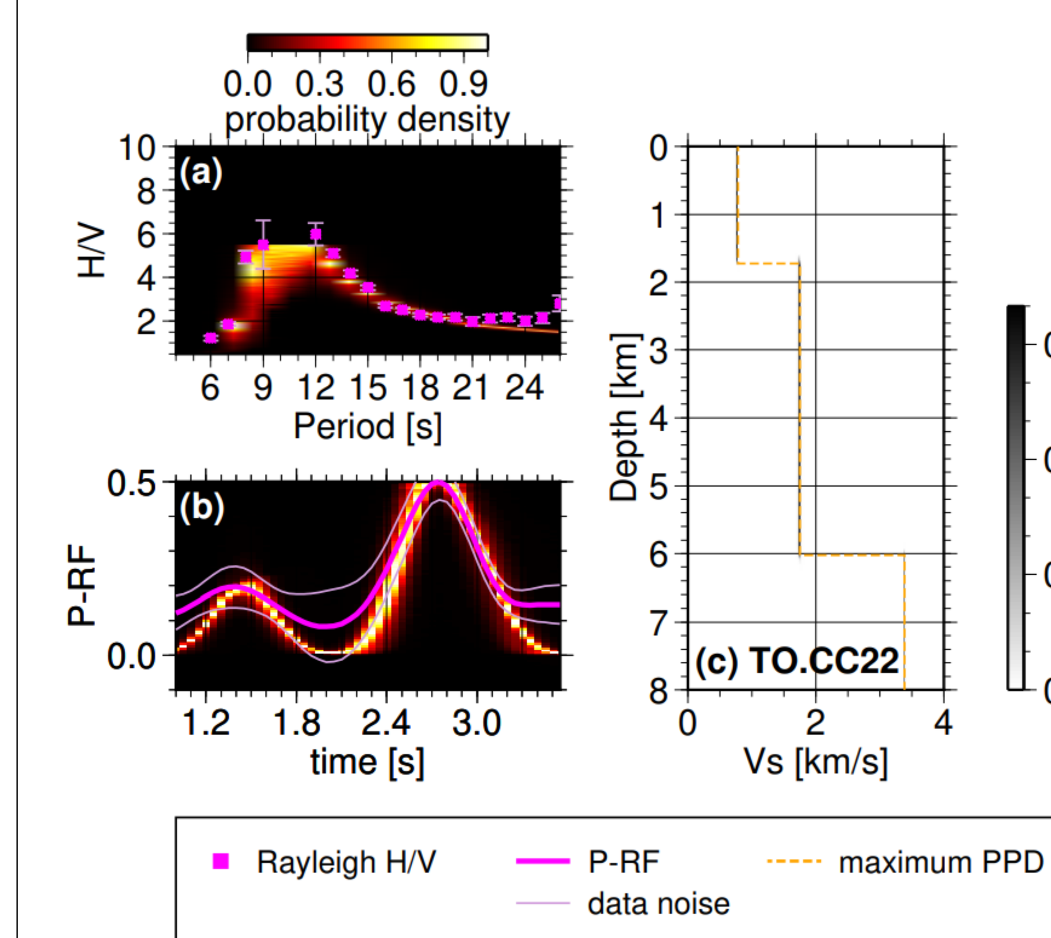

Figure 13: Example of Joint inversion of Rayleigh wave ellipticity and receiver function with Markov Chain Monte Carlo (MCMC) approach. (a) The observed (cyan) and predicted (red: probability density function from the MCMC inversion) Rayleigh wave H/V ratios. (b) Sam as (a) but for the receiver function. (c) The ensemble of models (i.e., posterior probability distribution from the MCMC approach) that fit the data (gray background). The orange line represents the maximum probability 1D Vs profile.

Acknowledgments

- Waveform data, metadata, and earthquake catalog for this study were accessed through the Northern California Earthquake Data Center (NCEDC). This project is partially supported by Southern California Earthquake Center.